

# Simulations of Planetary Ball Mill Using Discrete Element Method Modeling

MOHSEN MHADHBI

Laboratory of Useful Materials

National Institute of Research and Physicochemical Analysis

Technopole Sidi Thabet 2020 Ariana

TUNISIA

mohsen.mhadhbi@inrap.rnrt.tn

*Abstract:* - In recent years, the uses of computational techniques in the simulations of manufacturing processes design has increased considerably. Discrete element method (DEM) at the macroscale was used to simulate the motion of the balls and powders during milling in a planetary ball mill. It was concluded that the milling speed had the powerful effect on the media motion. An increase of the speed led to a change of the particles distribution. The obtained results show that the DEM simulations is a powerful tool to process optimization and equipment design.

*Key-Words:* - Ball mill, Simulations, Discrete Element Method (DEM), Modeling, Contact parameters, Particle breakage.

## 1 Introduction

Since a decade ago, several advances have been developed in understanding ball milling process, a considerable part of it concerning the application of the DEM simulations to numerically investigate the ball milling process for different ball mill models.

In 1970s, the DEM approach was developed by Cundall and Strack [1] to solve problems associated with rock mechanics. They used DEM simulations in the aim of distinguish the soft contacts model of finite duration from the event driven method. Moreover, Two and three dimensional DEM simulations of ball mill were primary reported by [2] and [3]. De Carvalho et al. [4] proposed a mechanistic model to describe grinding iron ore pellet feed in pilot and industrial scale ball mills by simulations using DEM. The obtained results showed a good agreement between predicted and measured size distributions and circulating load ratio. Hare et al. [5] compared the direct and indirect DEM-PBM ribbon milling size prediction approaches. It was concluded that the direct approach considers the shear deformation to be the governing breakage mechanism while the indirect approach considers the correct magnitude of fine

generation. Xie et al. [6] used DEM simulation to investigate an industrial semi-automatic grinding (SAG) mill with spherical grinding media and non-spherical ore based on polyhedron-sphere contact model. They revealed that the charging of particles in the polyhedron-sphere grinding was blocked to a certain extent and the collision energy between liner and ore was increased, which shows that the proposed model was necessary for more precise prediction of the grinding method. Similarly, Oliveira et al. [7] developed a mechanistic mill model for ball mills and used DEM to simulate breakage in a vertical stirred mill. The result showed good agreement between experimental and simulated particle size distribution for the case of limestone and copper ore, and small deviations was found (about 3.5 %). Additionally, the performance evaluation of the new multi-shaft mill using DEM was reported by Bracey et al. [8]. Thus, they concluded that the gravity fed material entering the multi-shaft mill. They also showed remarkable collisions, more than the critical breakage strength. Kushimoto et al. [9] developed a new ADEM-CFD model for analyzing dynamic and breakage behavior of aggregates in wet ball milling. They concluded that the proposed model can analyze the breakage

and dynamic characteristics of aggregates in wet ball milling.

DEM approach was used to simulate non-spherical particles using polyhedrons and super-ellipsoids during the grinding process of ore in a ball mill [10]. It was found that the proposed model was appropriate for the simulation of large scale systems and possess excellent stability. Cleary et al. [11] developed a new coupled DEM-SPH model to investigate the breakage and motion of resolved coarser particles in a semi-autogenous grinding (SAG) mill. They concluded that the new model was able to predict breakage and fine particle. Venugopal and Rajamani [12] revealed good agreement between 3D DEM simulation and experiments of charge motion in tumbling mill. They also concluded that DEM simulation could be include component lifetimes by following the impacts and position of impacts with mill shell and lifters over time. Govender et al. [13] used DEM approach to simulate the ball motion in wet milling. They concluded that the computational load could be reduced during the fluid flow simulation. The implementation of the combined DEM-BPM simulations was used to analyze the breakage of bonded agglomerates in a ball mill [14]. It was concluded that the computational simulations were a significant tool for analyzing the breakage and flow in ball mill. Bumeister et al. [15] determined the stressing conditions of dry grinding in planetary ball mills through DEM approach involving the contact model of Hertz and Mindlin. Thus, the correlation of breakage rates of powder and stressing conditions showed the influence of stressing on both breakage mechanism and breakage kinetics.

Additionally, frequency domain characterization of torque in tumbling ball mills through DEM modeling was reported by Pedrayes et al. [16]. The results showed the possibility of characterizing the load torque of ball mills in the frequency domain. It was also concluded that the load torque signal in ball mills involves sufficient information to characterize the load level of the ball mills. Furthermore, a combination of density-based clustering method and DEM were used to investigate the fragmentation of bonded particles

during the ball milling process [17]. It was showed that the collisions of balls expanded proportionally with rotation speed until achieving a critical rotation speed. It was also revealed that the mill power increase with increased rotation speed. Rodriguez et al. [18] analyzed the validity of some assumptions of advanced ball mill models by modelling through DEM simulations including particles and milling media. It was revealed that the supposition of perfect mixing in the radial direction was valid. It was also concluded that a fraction of the amount of collisions inner the mill does not require particles. DEM simulation of the charge motion and power draw of an experimental two-dimensional mill was developed by Van Nierop et al. [19]. It was found, based on DEM simulations runs, that at super-critical speeds, the centrifuging of material in the load was predicted. In our previous work [20], we studied the simulation of high-energy ball milling process by using DEM modelling approach. The simulations results showed the efficiency of mechanical alloying process for low velocities ratios.

In this paper, we describe DEM simulations of dry ball milling, including initial conditions, calibration, and validation.

## 2 Post processing of DEM simulations

DEM is a particle based approach where each particle in the flow is tracked and all collisions between particles and between particles and boundaries are modeled using a contact force law.

### 2.1 Contact dynamic model

The contact models are based on theories of contact between particles with spherical shape. Thus, a non-linear bringing together Hertz's theory in the normal direction and the improvement to Mindlin's no-slip model [21] in the tangential direction was used for modeling (Fig. 1). In fact, Hertz's theory of elastic contacts describes which are derived among integration of the normal stress distribution in the contact area [22].

Therefore, the resulting total force, as a sum of elastic and dissipative forces, is expressed by [23]:

$$F_n = -k_n \delta_n + C_n \dot{g}_n^{rel} \quad (1)$$

where  $k_n$  is the normal spring stiffness constant ( $k_n = \frac{4}{3} E^* \sqrt{R^* \delta_n}$ ),  $\delta_n$  is the amount of overlap,  $C_n$  is the normal damping coefficient ( $C_n = 2 \sqrt{\frac{5}{6}} \beta \sqrt{S_n m^*}$ ), and  $\mathcal{G}_n^{rel}$  is the relative normal velocity from the relative tangential motions over the collision.

However, average overlap of 0.1-0.5 % of the particles diameter and spring constant of 106-108  $\text{Nm}^{-1}$  are recommended.

In hence, the dashpot dissipates energy resulting from the tangential motion and models the plastic deformation because of contact in the tangential direction [24, 25]. Thus, the tangential force-displacement is dependent on normal and tangential loading history.

The total tangential force which is limited by Coulomb's law of friction [22, 23] is given by:

$$F_t = \min \{ \mu F_n, k_t \delta_t + C_t \mathcal{G}_t^{rel} \} \quad (2)$$

where  $k_t$  is the tangential spring stiffness constant ( $k_t = 8G^* \sqrt{R^* \delta_n}$ ),  $C_t$  is the tangential damping coefficient ( $C_t = 2 \sqrt{\frac{5}{6}} \beta \sqrt{k_t m^*}$ ),  $\mu$  is the friction coefficient, and  $\mathcal{G}_t^{rel}$  is the relative tangential velocity. The integral of the tangential velocity over the relative behaves as an incremental spring that stores energy from the relative tangential motions.

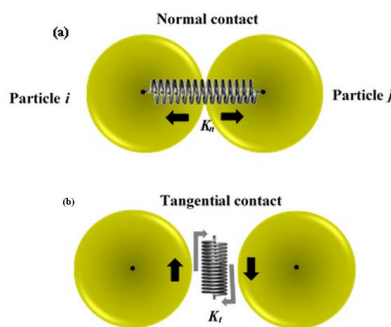


Figure 1. Graphic representation of the DEM contact model between two particles.

### 2.2 Wear model

During collision event, the balls and particles hitting generate wear on the liner/lifter surface. In consequence, the total volume lost due to adhesive wear. This loss may be given by:

$$\Delta V = d \mathcal{G} t h \quad (3)$$

where  $\Delta V$  is the wear track volume,  $d$  is the wear track width,  $\mathcal{G}$  is the velocity,  $t$  is the time, and  $h$  is the depth of the wear track.

Moreover, for simplicity the DEM simulations, we use the average values of velocity and loading through the whole duration of a wear contact phenomena. This results in the supposition that the parameters are constant through the duration of impact.

It also may be assumed that the wear track depth depends of the applied compressive force, sliding distance, which equal velocity times sliding time [26]:

$$h = f(F_n, \mathcal{G} t) \quad (4)$$

Therefore, the wear track width is inversely proportional to materials hardness. We can combine Eq (3) and Eq (4):

$$\Delta V = \frac{k d}{H_B} F_n \mathcal{G} t \quad (5)$$

In the DEM simulations, the liner is meshed into a series of surface elements from which the whole surface is created. Thus, during modeling the mesh should be correctly chosen to obtain logical elements for wear modeling.

The total volume loss in a selected region on a liner or lifter during an identified revolution of the ball mill is the addition of all the event based volume losses as:

$$V_{el} = \sum_{rev} \Delta V_i \quad (6)$$

In hence, the total volume loss may be transformed to a height loss as follows:

$$\Delta H_{el} = \frac{V_{el}}{A_{el}} \quad (7)$$

However, various approaches were used to wear modeling.

### 2.3 Capture of particles between milling media

Fig. 2 shows the collision event between two milling media (balls) and a number of captured particles in the milling zone relative to the stress energy, based on surface and mechanical properties. At elevated flow ability, the material (particles)

captured in the milling zone (between two balls) is too low, resulting a low efficiency [27]. In fact, the reduction in the surface energy is one of the main influential factors on milling.

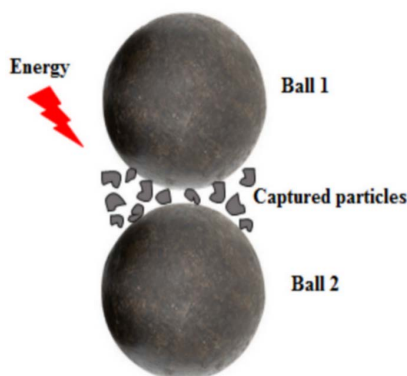


Fig. 2. Schematic of the particles capturing between milling media.

### 3 Ball mill configuration and DEM simulations parameters

The ball mill used in this study is a planetary ball mill at laboratory scale. The powders distribution, the balls distribution, and the wear were modeled using EDEM software [28]. The simulations of dry mill were conducted by using a standard coefficient of restitution of 0.3 and a friction coefficient of 0.75 (ball-ball and ball-liner collisions) [29]. Furthermore, the charge consisted of powders and balls with filling of 40 % of the whole volume. The materials properties used in the simulations are presented in Table 1.

Table 1. Materials properties used in the simulations.

Parameter	Value
Poisson's ratio	0.3
Young's modulus (N/m <sup>2</sup> )	1.8×10 <sup>11</sup>
Density (kg/m <sup>3</sup> )	7700

In hence, the ball mill parameters are illustrated in Table 2. The specific gravity of the media is equal to 2.7. During DEM simulations, the geometry and the motion are easy and the media are considered and represented as a spherical element.

Table 2. Ball mill parameters.

Parameter	Value
-----------	-------

Shaft power (kW)	0.37
Angular speed (used here) (rpm)	250
Effective diameter of main disc (mm)	140
Mill filling (%)	40
Mill speed (% critical speed)	10-100
Time step (s)	1.01×10 <sup>-4</sup>
Ball density (kg/m <sup>3</sup> )	7700
Vial density (kg/m <sup>3</sup> )	7700
Length (mm)	370
Depth (mm)	530
Height (mm)	500
Weight (kg)	50

### 4 DEM simulations results

DEM simulations describe the collisions between milling media occurred in the mill by given collision energy spectrum.

Fig. 3 shows the different stages of particles breakage during simulations of ball milling. As can be seen from all the figures (a-f), the powders distribution is mainly concentrated near the wall of vial due to the high centrifugal accelerations caused by the motion of the vial. However, in the case of run simulation between 2 and 3 s, we observed that the simulation behavior remains almost unchanged. Beside between 4 and 5 s a particles clumping was occurred. For extended time between 6 and 7 s, the run simulation the particles motion reached a steady state. In fact, the results confirm that time is a very important factor which influences the changing behavior of the particles during milling.

In addition, with an increase in time, the particles occupy nearly the entire volume of vial space. In hence, the smaller particles, which receive large amount of the impact energy, circulate on closed trajectories near the wall of vial due to gravity [30]. Furthermore, the velocity coloring (from blue: slow to red: fast) provides information on the charge motion. It would be also considered that the number of collisions decreases with increasing energy per collision [31].

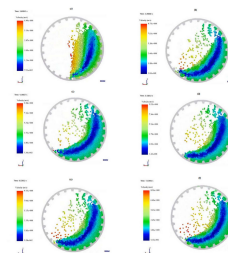


Fig. 3. Snapshots of a ball mill at different stages of particles breakage: (a) t = 2 s, (b) t = 3 s, (c) t = 4 s, (d) t = 5 s, (e) t = 6 s, and (f) t = 7 s.

Fig. 4 shows the variation of the number of particles contact with time. The particle to particle contact

graph exhibits that the number of contacts increases over time. This increase is related to the increase of velocity.

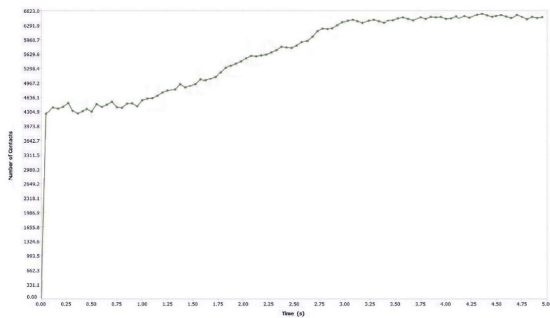


Fig. 4. Variation of number of particles contact with time.

## 5 Conclusion

In this work, milling process with different parameters was simulated through DEM approach. The results showed that the milling speed had a significant effect on the media motion. The proposed model is applicable to any other particulate process where there are notable amounts of fine material that influence the process. Finally, it is revealed that this numerical model is a powerful tool for knowledge and understanding of dry milling media in ball mills.

### References:

- [1] P.A. Cundall, O.D.L. Strack, A discrete numerical model for granular assemblies, *Geotechnique*, Vol. 29, No 1, 1979, pp. 47-65.
- [2] B.K. Mishra, R.K. Rajamani, The discrete element method for the simulation of ball mills, *Applied Mathematical Modelling*, Vol. 16, No 11, 1992, pp. 598-604.
- [3] P.W. Cleary, M.L. Sawley, Three-dimensional modelling of industrial flows, *Second International Conference on CFD in the Minerals and Process Industries*, CSIRO, Melbourne, Australia, 1999.
- [4] R.M. de Carvalho, T.M. Campos, P.M. Faria, L.M. Tavares, Mechanistic modeling and simulation of grinding iron ore pellet feed in pilot and industrial-scale ball mills, *Powder Technology*, Vol. 392, 2021, pp. 489-502.
- [5] C. Hare, M. Ghadiri, C.Y. Wu, Discrete element modelling of ribbon milling: A comparison of approaches, *Powder Technology*, Vol. 388, 2021, pp. 63-69.
- [6] C. Xie, H. Ma, T. Song, Y. Zhao, DEM investigation of SAG mill with spherical grinding media and non-spherical ore based on polyhedron-sphere contact model, *Powder Technology*, Vol. 386, 2021, pp. 154-165.
- [7] A.L.R. Oliveira, V.A. Rodriguez, R.M.de Carvalho, M.S. Powell, L.M. Tavares, Mechanistic modeling and simulation of a batch vertical stirred mill, *Minerals Engineering*, Vol. 156, 2020, pp. 106487
- [8] R.J. Bracey, N.S. Weerasekara, M.S. Powell, Performance evaluation of the novel multi-shaft mill using DEM modelling, *Minerals Engineering*, Vol. 98, 2016, pp. 251-260.
- [9] K. Kushimoto, S. Ishihara, J. Kano, Development of ADEM-CFD model for analyzing dynamic and breakage behavior of aggregates in wet ball milling, *Advanced Powder Technology*, Vol. 30, No 6, 2019, pp. 1131-1140.
- [10] C. Xie, T. Song, Y. Zhao, Discrete element modeling and simulation of non-spherical particles using polyhedrons and super-ellipsoids, *Powder Technology*, Vol. 368, 2020, pp. 253-267.
- [11] P.W. Cleary, R.D. Morrison, M.D. Sinnott, Prediction of slurry grinding due to media and coarse rock interactions in a 3D pilot SAG mill using a coupled DEM + SPH model, *Minerals Engineering*, Vol. 159, No 1, 2020, pp.106614.
- [12] R. Venugopal, R.K. Rajamani, 3D simulation of charge motion in tumbling mills by the discrete element method, *Powder Technology*, Vol. 115, No 2, 2001, pp. 157-166.
- [13] I. Govender, P.W. Cleary, A.N. Mainza, Comparisons of PEPT derived charge features in wet milling environments with a friction-adjusted DEM model, *Chemical Engineering Science*, Vol. 97, 2013, pp. 162-175.
- [14] J.M. Metzger, B.J. Glasser, Simulation of the breakage of bonded agglomerates in a ball mill, *Powder Technology*, Vol. 237, 2013, pp. 286-302.
- [15] C. Burmeister, L. Titscher, S.B.F. Arno Kwade, Dry grinding in planetary ball mills: Evaluation of a stressing model, *Advanced Powder Technology*, Vol. 29, No 1, 2018, pp. 191-201
- [16] F. Pedrayes, J.G. Norriella, M.G. Melero, J.M. Menéndez-Aguado, J.J. del Coz-Díaz, Frequency domain characterization of torque in tumbling ball mills using DEM modelling:

- Application to filling level monitoring, *Powder Technology*, Vol. 323, No1, 2018, pp. 433-444.
- [17] A. Krok, P. Peciar, K. Coffey, K. Bryan, S. Lenihan, A combination of density-based clustering method and DEM to numerically investigate the breakage of bonded pharmaceutical granules in the ball milling process, *Particuology*, Vol. 58, 2021, pp. 153-168.
- [18] A.V. Rodriguez, R.M. de Carvalho, L.M. Tavares, Insights into advanced ball mill modelling through discrete element simulations, *Minerals Engineering*, Vol. 127, 2018, pp. 48-60.
- [19] M.A. Van Nierop, G. Glover, A.L. Hinde, M.H. Moys, A discrete element method investigation of the charge motion and power draw of an experimental two-dimensional mill, *Processing*, Vol. 61, No 2, 2001, pp. 77-92.
- [20] M. Mhadhbi, Modelling of the High-Energy Ball Milling Process, *Advances in Materials Physics and Chemistry*, Vol. 11, 2021, pp. 31-44.
- [21] R.D. Mindlin, Compliance of elastic bodies in contact. *Journal of Applied Mechanics*, Vol. 16, 1949, pp. 259-268.
- [22] A.D. Renzo, F.P.D. Maio, Comparison of contact-force models for the simulation of collisions in DEM-based granular flow codes. *Chemical Engineering Science*, Vol. 59, 2004, pp. 525-541.
- [23] P.W. Cleary, Predicting charge motion, power draw, segregation and wear in ball mills using discrete element methods, *Minerals Engineering*, Vol. 11, No 11, 1998, pp. 1061-1080.
- [24] S.B. Yeom, E.S. Ha, M.S. Kim, S.H. Jeong, S.J. Hwang, D.H. Choi, Review on Application of the Discrete Element Method for Manufacturing Process Simulation in the Pharmaceutical Industry, *Pharmaceutics*, Vol. 11, 2019, pp. 414.
- [25] M.S. Powell, N.S. Weerasekara, S. Cole, R.D. LaRoche, J. Favier, DEM modelling of liner evolution and its influence on grinding rate in ball mills, *Minerals Engineering*, Vol. 24, 2011, pp. 341-351.
- [26] P. Radziszewski, R. Varadi, T. Chenje, L. Santella, A. Sciannamblo, Tumbling mill steel media abrasion wear test development, *Minerals Engineering*, Vol.18, No 3, 2005, pp. 333-341.
- [27] V. Chipakwe, P. Semsari, T. Karlkvist, J. Rosenkranz, S. Chehreh Chelgani, A critical review on the mechanisms of chemical additives used in grinding and their effects on the downstream processes, *Journal of Materials Research and Technology*, Vol. 9, 2020, pp.8148-8162.
- [28] <https://www.edemsimulation.com/software/>
- [29] P.W. Cleary, Charge behaviour and power consumption in ball mills: sensitivity to mill operating conditions, liner geometry and charge composition, *International Journal of Mineral Processing*, Vol. 63, 2001, pp. 79-114.
- [30] F. Hirose, T. Iwasaki, M. Iwata, Particle impact energy variation with the size and number of particles in a planetary ball mill, *MATEC Web of Conferences*, Vol. 333, 2021, pp. 1-5.
- [31] D. Daraio, J. Villoria, A. Ingram, A. Alexiadis E.H. Stitt, A.L. Munnoch, M. Marigo, Using Discrete Element method (DEM) simulations to reveal the differences in the  $\gamma$ -Al<sub>2</sub>O<sub>3</sub> to  $\alpha$ -Al<sub>2</sub>O<sub>3</sub> mechanically induced phase transformation between a planetary ball mill and an attritor mill, *Minerals Engineering*, Vol. 155, 2020, pp. 106374.

#### Author Contributions:

Mohsen Mhadhbi carried out the simulation, the optimization, and wrote the paper throughout.

#### Sources of funding for research presented in a scientific article or scientific article itself

No funding to declare.